12 月 December
2020, 63(12): 1525 – 1535
昆 虫 学 报
ACTA ENTOMOLOGICA SINICA
http://www.insect.org.cn
doi: 10.16380/j.kcxb.2020.12.011

Genetic differentiation and phylogeography of the pierid butterfly *Colias fieldii* (Pieridae: Coliadinae) in China based on mitochondrial gene sequences

CHEN Ke-Ke[1], LUO A-Rong[2], WANG Yun-Liang[1], SI Cheng-Cai[1], HUANG Dun-Yuan[3], SU Cheng-Yong[1], HAO Jia-Sheng[1,*], ZHU Chao-Dong[2,*]

(1. College of Life Sciences, Anhui Normal University, Wuhu, Anhui 241000, China; 2. Key Laboratory of Zoological Systematics and Evolution, Institute of Zoology, Chinese Academy of Sciences, Beijing 100101, China; 3. College of Life Sciences, Chongqing Normal University, Chongqing 401331, China)

Abstract: 【Aim】This study aims to explore the genetic diversity, genetic differentiation, and phylogenetic relationships among populations of the pierid butterfly *Colias fieldii* in China, to infer their origin and divergence time, and to preliminarily clarify the causes of their spatiotemporally evolutionary history. 【Methods】The four mitochondrial gene (*COI*, *Cytb*, *NDI* and *ND5*) sequences of 115 individuals from 23 geographic populations of *C. fieldii* in China collected in 2006 – 2018 were amplified by PCR and sequenced. The genetic diversity and genetic differentiation were analyzed using MEGA v.7.0, DnaSP v.5.0, Arlequin v.3.5.1 and other genetic analysis software. Using the closest relatives as the outgroups, the phylogenetic trees and haplotype median-joining network of *C. fieldii* were reconstructed with such analytical software as IQ-TREE, MrBayes v.3.1.2, Network v.4.6 and BEAST v.1.8.3, and the origin and divergence time of *C. fieldii* were estimated by using relaxed molecular dating method and calibrations of the previous studies. Based on the present biogeographic distribution of *C. fieldii* and the main earth environmental events since the Quaternary Period, the spatio-temporal pattern of its biogeographic distribution and the underlying earth environmental factors were tentatively inferred. 【Results】The aligned sizes of mitochondrial gene segments of *COI*, *Cytb*, *NDI* and *ND5* of *C. fieldii* populations are 648, 699, 393 and 777 bp, respectively, and the concatenated sequence of the four genes is 2 517 bp in length, which was shown to be significantly AT biased. In total, 18 haplotypes based on the four mitochondrial gene sequences were found in 115 individuals of 23 geographic populations of *C. fieldii*, with the haplotype diversity (*Hd*) of 0.677 ± 0.048 and nucleotide diversity (π) of 0.00066 ± 0.00007 of the total population, showing a relatively high level of haplotype diversity and a low level of nucleotide diversity. The phylogenetic analysis showed that 18 haplotypes of *C. fieldii* populations were distinctly categorized into two large clades (clade I and II). Clade I included 13 haplotypes of populations from Shaanxi, Henan, Gansu, Anhui, Hubei, Sichuan, Qinghai, and some regions of Yunnan. Clade II included five haplotypes of populations from some regions of Yunnan and Tibet. The results of reconstructed haplotype median-joining network were generally consistent with those of the phylogenetic tree. AMOVA analysis indicated that a larger level of population differentiation (64.36%) occurred between the two haplotype clades and a subtle genetic differentiation (35.64%) existed within each haplotype clade of *C. fieldii*. The analysis results of neutrality tests and mismatch distribution indicated that populations with haplotypes in clade I did not experience a population expansion event, whereas those with haplotypes in clade II probably had a sudden demographic expansion at about 0.085 Ma in the late Pleistocene, a little earlier than the Last Glacial Maximum event, which may be caused by the warm and humid plateau climate in the interglacial period, the expansion of forest grassland and the decreased heavy rainfall on the core plateau. 【Conclusion】The genetic differentiation of *C. fieldii* populations is correlated significantly with the geographical distance. In addition, we proposed that *C. fieldii* populations originated at about 0.48 Ma in southwestern areas of China (presently the Hengduan Mountains and adjacent areas), and began to diversify into two clades and later dispersed into other low-latitude areas due to the Quaternary glacial-interglacial cycle events, Southeast Asia monsoon and different habitat environments.

Key words: *Colias fieldii*; genetic differentiation; haplotype; mitochondrial gene; molecular dating; phylogeography; China

基金项目: 国家科技基础资源调查专项课题(2018FY100405); 国家自然科学基金项目(41172004, 41472028)

作者简介: 陈可可, 女, 1992 年 8 月生, 安徽蚌埠人, 硕士研究生, 研究方向为昆虫分子系统学与进化, E-mail: chenkeke0917@163.com

*通讯作者 Corresponding authors, E-mail: jshaonigpas@sina.com; zhucd@ioz.ac.cn

收稿日期 Received: 2020-05-29; 接受日期 Accepted: 2020-08-12

1 INTRODUCTION

Colias fieldii is one pierid butterfly species commonly found and distributed in Central Asia, inhabiting at areas of grassy and wooded steppes (Laiho and Ståhls, 2013; Ding and Zhang, 2017). As one of the important pollinator insects, it plays a critical role in plant reproduction (Yang *et al.*, 2019). Previous morphological and ecological studies have provided much useful evidence for taxonomy and phylogeny of this species and related taxa (Meng *et al.*, 2013). In recent decades, more researchers attempted to investigate the relevant studies by using molecular data criteria. For example, Wheat and Watt (2008) reconstructed the molecular phylogenetic relationships of North American *Colias* taxa using mitochondrial genes, and their results suggested that molecular divergences among the *Colias* species were relatively small. Schoville *et al.* (2011) studied the evolutionary history of *Colias behrii*, showing that *C. behrii* had a very low level of genetic diversity at mitochondrial and nuclear loci. However, this study did not explore the impacts of Quaternary glacial period on distribution and genetic structure of the *Colias* species in the Qinghai-Tibet Plateau (QTP).

The Qinghai-Tibet Plateau (QTP) in China, recognized as the world's third pole, is the highest and largest plateau in the world with an average elevation of about 4 000 m and an area of about 2.5 million km^2. Because of its high elevation and specific climate, this plateau dramatically affects terrestrial fauna and ecosystems in western China and the neighboring areas. Specifically, the rapid uplift of the QTP between 1.1 and 0.6 Ma gave rise to the average altitude and initiated widespread mountain glaciers during the ice ages (Zheng, 1996; Zhou *et al.*, 2006; Favre *et al.*, 2015). The topographic variation of the QTP, including the forming of the Hengduan Mountains, coupled with cyclical climatic changes, namely the alternating glacial-interglacial periods in the Pleistocene exerted enormous influences on the current spatial distribution and genetic structure of many resident species (Cao *et al.*, 2012; Li *et al.*, 2012). Previous studies have demonstrated that the geological events as well as accompanying environmental changes might have caused rapidly evolutionary radiation of many insect groups (Gratton *et al.*, 2008). *C. fieldii* is also found in the QTP, and its genetic differentiation is closely related to the environmental background of the QTP.

Due to lack of recombination, maternal inheritance and other merits compared with nuclear genes, mitochondrial DNA (mtDNA) genes have been widely used to study molecular evolution, phylogenetics, and population genetics in animals for several decades (Galtier *et al.*, 2009). The cytochrome oxidase subunit I (COI) gene is relatively conservative and widely used in inferring inter- and intra-species phylogenetic relationships, and the cytochrome b (Cytb) gene has a moderate rate of molecular evolution, being suitable to clarify the phylogenetic relationships between families, genera, species and even populations of a single species. In addition, the mitochondrial genes dehydrogenase subunit 5 gene (*ND5*) and dehydrogenase subunit I gene (*NDI*) which harbor a relatively fast evolutionary rates, are suitable for resolving relatively lower level relationships (Cameron, 2014; He *et al.*, 2016; Su *et al.*, 2017). In recent decades, combined mitochondrial dataset was often utilized to investigate the genetic differentiations and phylogenetic relationships among insects at the inter- and intra-species level (Tao *et al.*, 2020).

In this study, we firstly determined the sequences of four mitochondrial genes (*COI*, *Cytb*, *NDI* and *ND5*) of total 115 individuals of 23 populations of *C. fieldii* from the Qinghai-Tibet Plateau and other areas in China. Based on these datasets of four mitochondrial gene sequences, we analyzed their genetic differentiation among populations, assessed their phylogeographic structure using a variety of genetic diversity analysis methods, and analyzed their demographic history using the mismatch distribution and neutrality test analysis methods, reconstructed their phylogenetic trees, and estimated the divergence time of their main lineages with relaxed molecular dating methods. In general, we aim to clarify their divergence timescales and the related geological and environmental events in the evolutionary history of *C. fieldii*.

2 MATERIALS AND METHODS

2.1 Sample collection and DNA extraction

We collected 115 adult individuals of *C. fieldii* from 23 sampling sites in central and southwestern China. Sample size and geographical coordinates for each population were shown in Table 1. After species identification, the fresh thorax muscle tissues were immediately preserved in 100% ethanol for DNA fixation and stored at −20℃ for further genomic DNA isolation. Total genomic DNA was extracted from thorax muscle using a DNA extraction kit (Sangon Biotech, Shanghai) according to the

manufacturer's instructions.

2.2 PCR amplification and sequencing

Four mitochondrial gene (*COI*, *Cytb*, *NDI*, and *ND5*) fragments were amplified by using standard short primers (Simon *et al.*, 1994; Yagi *et al.*, 1999). All primers were synthesized by Sangon Biotech (Shanghai) shown in Table 2. PCR was performed in a PCR reaction (50 μL) of genomic DNA (20 ng/mL) 1.5 μL, 10 × Buffer 6.0 μL, Mg^{2+} (25 mmol/L) 8.0 μL, dNTPs (0.2 mmol/L) 1.5 μL, Taq DNA polymerase 0.6 μL, 1.8 μL of each of the primers (1.0 ng/mL), and ddH_2O 28.8 μL, under the following conditions: an initial denaturation at 95℃ for 5 min; 35 cycles of denaturation at 94℃ for 50 s, annealing at 46 – 52℃ (depending on the primer pairs) for 50 s, and extension at 72℃ for 120 s; and a final extension at 72℃ for 10 min. The PCR products were sequenced on an ABI-377 automatic DNA sequences (Sangon Biotech, Shanghai).

Table 1 Sampling information, haplotype diversity and nucleotide diversity estimated based on mitochondrial genes *COI*, *Cytb*, *NDI*, and *ND5* of *Colias fieldii* populations in China in this study

Population	Locality	Sample size	Longitude and latitude	Haplotype (number of individuals)	Haplotype diversity *Hd*	Nucleotide diversity π
BJ	Baoji, Shaanxi	5	33.35°N, 106.18°E	A1(1), A15(4)	0.400	0.00016
BMS	Bamishan, Gansu	5	35.53°N, 103.25°E	A15(5)	0	0
HBY	Huangbaiyuan, Shaanxi	5	33.73°N, 107.40°E	A5(4), A15(1)	0.400	0.00016
LY	Luoyang, Henan	5	33.35°N, 111.8°E	A15(5)	0	0
ELS	Elashan, Qinghai	5	34.07°N, 103.41°E	A4(4), A15(1)	0.520	0.00052
GN	Guanggaishan, Gansu	5	34.13°N, 103.17°E	A15(5)	0	0
KJM	Kajiaman, Gansu	5	35.05°N, 102.52°E	A6(4), A15(1)	0.400	0.00016
HF	Hefei, Anhui	5	31.30°N, 117.14°E	A15(5)	0	0
SY	Shiyan, Hubei	5	32.65°N, 110.79°E	A15(5)	0	0
JZG	Jiuzhaigou, Sichuan	5	34.19°N, 104.27°E	A15(5)	0	0
SNJ	Shennongjia, Hubei	5	31.21°N, 110.03°E	A15(5)	0	0
QCS	Qingchengshan, Sichuan	5	30.54°N, 103.35°E	A10(1), A11(1), A12(1), A15(2)	0.900	0.00079
LJ	Lijiang, Yunnan	5	26.86°N, 100.25°E	A3(1), A7(2), A15(1)	0.800	0.00087
DQ	Deqin, Yunnan	5	29.15°N, 99.32°E	A3(2), A15(3)	0.600	0.00119
DL	Dali, Yunnan	5	26.42°N, 101.03°E	A2(3), A7(2)	0.600	0.00048
MK	Mangkang, Tibet	5	30.20°N, 99.05°E	A15(5)	0	0
XLZ	Linzhi, Tibet	5	30.20°N, 91.24°E	A18(5)	0	0
LS	Lhasa, Tibet	5	29.97°N, 91.11°E	A14(5)	0	0
SFG	Shifogou, Gansu	5	36.12°N, 103.45°E	A13(2), A15(3)	0.600	0.00095
LZ	Lanzhou, Gansu	5	36.03°N, 103.40°E	A8(1), A9(2), A15(2)	0.800	0.00040
XY	Yangling, Shaanxi	5	34.20°N, 107.59°E	A15(5)	0	0
ZQ	Zhaqi, Tibet	5	29.28°N, 91.26°E	A16(1), A17(2), A18(2)	0.800	0.00064

Table 2 PCR primers used in this study

Gene	GenBank accession no.	Primer sequences (5′–3′)	Annealing temperature (℃)
COI	MN29887 – MN298986	F: GGTCAACAAATCATAAAGATATTG R: TAAACTTCAGGGTGACCAAAAAT	46.8
Cytb	MN305324 – MN305438	F: TACGTTTTACCATGAGGTCAAATAC R: ACTTCTTTTCTTATGTTTTCAAAAC	52.2
NDI	MN305439 – MN305553	F: ACATGAATTGGAGCTCGACCAGT R: ACATGATCTGAGTTCAAACCGG	52
ND5	MN305554 – MN305668	F: CCTGTTTCTGCTTTAGTTCA R: AATATDAGGTATAAATCATAT	52.8

2.3 Phylogenetic analysis

Using *Gonepteryx rhamni* and *Eurema hecabe* as the outgroups, phylogenetic trees were reconstructed with the Bayesian inference (BI) and maximum likelihood (ML) methods based on different mitochondrial datasets. The jModelTest v. 2. 0

(Darriba *et al.*, 2012) was used to select the GTR + I + G model as the best-fit substitution model of molecular evolution. BI analysis using the Markov chain Monte Carlo (MCMC) method was performed by MrBayes v. 3. 1. 2 (Huelsenbeck and Ronquist, 2001; Ronquist and Huelsenbeck, 2003). ML analysis was carried out in IQ-TREE v. 1. 6. 8 under the GTR + I + G model (Nguyen *et al.*, 2014; Zhang *et al.*, 2018). Finally, a ML tree in NEWICK format was visualized by FigTree v. 1. 4. 3 (Rambaut, 2009). In addition, median-joining network of haplotypes was constructed with Network v. 4. 6 (Bandelt *et al.*, 1999). The phylogeographic structure was tested by calculating two indices of genetic differentiation G_{ST} and N_{ST} using DnaSP v. 5. 0 (Pons and Petit, 1996; Librado and Rozas, 2009). The genetic differentiation coefficient (F_{ST}) and gene flow (Nm) were calculated using Arlequin v. 3. 5. 1 (Excoffier and Lischer, 2010). Analysis of molecular variance (AMOVA) was performed to distinguish variations within and among populations, with significance tested via 1 000 nonparametric permutations.

2.4 Population demographic analysis

To infer population demographic history of *C. fieldii*, Tajima's D (Tajima, 1989) and Fu's F_S (Fu, 1997) were calculated using Arlequin v. 3. 5. 1. In addition, mismatch distribution was used to identify historical processes between recent demographic expansion and population equilibrium (Rogers and Harpending, 1992; Cristiano *et al.*, 2016). The validity of the two models fitting to our data was assessed by the sum of squared deviation (SSD) and Harpending's raggedness index (HRI) (Harpending, 1994). The time of population expansion (t, time in generations) was then estimated using the formula $\tau = 2ut$ (You *et al.*, 2010), where τ was the mode of mismatch distribution and u was the mutation rate per generation for the entire sequences under this study (the value of u was calculated using the equation $u = \mu k$, where μ was the mutation rate per nucleotide per generation and k was the number of nucleotides assayed).

2.5 Divergence time estimation analysis

Based on the 18 haplotypes, using *Artogeia melete*, *Pieris rapae*, *Aporia intercostata* and *Aporia hippia* as the outgroups, *C. fieldii* of this study and their related taxa of *C. montium*, *C. erate*, *C. croceus*, *Catopsilia pomona*, *Gonepteryx mahaguru*, *Gonepteryx rhamni*, and *Eurema hecabe* were used to reconstruct the species tree and estimate the divergence time simultaneously using the BEAST v. 1. 8. 3 (Drummond and Rambaut, 2007). Uncorrelated relaxed clocks were used to estimate the branch lengths, with the tree prior of the birth-death process, and the nucleotide substitution model was set to the GTR + G model. The oldest Pieridae fossils *Stolopsyche libytheoidea* and *Coliates proserpina* were selected for fossil calibrations, and thus the minimum age of the genus *Pieris* and the genus *Aporia* were constrained to be 37. 2 – 33. 9 Ma and 33. 5 – 30 Ma, respectively (Scudder, 1875, 1889; Braby and Trueman, 2006). In addition, according to insect-host plant coevolutionary scenario and the molecular dating of the Brassicales' s radiation, the earliest divergence time of Coliadinae and Pierinae was set to be 90 – 85 Ma. The convergence of the MCMC chains was evaluated by ESS values above 200 in Tracer v. 1. 7. 1 (Rambaut *et al.*, 2018). The maximum-clade-credibility tree was finally visualized and edited in FigTree v. 1. 4. 3 (Carneiro *et al.*, 2018).

2.6 Data analysis

The mitochondrial gene sequences of *COI*, *Cytb*, *NDI*, and *ND5* from all individuals of *C. fieldii* were aligned via MAFFT v. 7. 1 (Katoh *et al.*, 2017) and concatenated by DAMBE v. 6. 0 (Xia, 2017). The nucleotide composition of the mitochondrial gene sequences was analyzed by MEGA v. 7. 0 (Kumar *et al.*, 2016). The haplotype diversity (Hd), haplotype number (h), and nucleotide diversity (π) were calculated using DnaSP v. 5. 0 (Librado and Rozas, 2009).

3 RESULTS

3.1 Genetic diversity

Four mitochondrial genes including partial *COI* (648 bp), *Cytb* (699 bp), *NDI* (393 bp) and *ND5* (777 bp) were amplified and obtained, and the concatenated sequence of the four genes is 2 517 bp in length. The obviously AT-biased dataset with no indels or stop codons totally contained 18 haplotypes (A1 – A18) (Table 3), among which six were unique haplotypes, each found only in one population, and the remaining twelve haplotypes were shared among two or more different populations. The most abundant haplotype A15, shared by 64 individuals, was distributed in 18 populations (Table 1). The calculated haplotype diversity (Hd) and nucleotide diversity (π) of the whole population were 0. 677 ± 0. 048 and 0. 00066 ± 0. 00007, respectively, with the haplotype diversity and nucleotide diversity of each geographic population shown in Table 1.

Table 3　Characteristics of haplotypes based on the concatenated sequence of mitochondrial genes *COI*, *Cytb*, *NDI* and *ND5* of *Colias fieldii* populations in China

Haplotype	T(U)	C	A	G	Total	AT-skew	GC-skew
A1	43.6	11.4	33.1	11.9	2517.0	−0.1368	0.0221
A2	43.6	11.4	33.1	11.9	2517.0	−0.1368	0.0221
A3	43.5	11.4	33.2	11.9	2517.0	−0.1352	0.0205
A4	43.6	11.4	33.1	12.0	2517.0	−0.1374	0.0238
A5	43.7	11.3	33.1	11.9	2517.0	−0.1377	0.0256
A6	43.6	11.4	33.1	11.9	2517.0	−0.1368	0.0221
A7	43.6	11.4	33.1	11.9	2517.0	−0.1368	0.0221
A8	43.6	11.4	33.1	11.9	2517.0	−0.1366	0.0222
A9	43.6	11.4	33.1	11.9	2517.0	−0.1366	0.0222
A10	43.6	11.4	33.1	11.9	2517.0	−0.1368	0.0221
A11	43.6	11.4	33.1	11.9	2517.0	−0.1362	0.0239
A12	43.6	11.4	33.1	11.9	2517.0	−0.1366	0.0222
A13	43.6	11.4	33.1	11.9	2517.0	−0.1362	0.0205
A14	43.6	11.4	33.2	11.8	2517.0	−0.1356	0.0188
A15	43.6	11.4	33.1	11.9	2517.0	−0.1372	0.0239
A16	43.6	11.4	33.1	11.9	2517.0	−0.1362	0.0205
A17	43.5	11.4	33.2	11.8	2517.0	−0.1352	0.0171
A18	43.6	11.4	33.2	11.8	2517.0	−0.1361	0.0205

3.2　Phylogenetic analysis

Our phylogenetic analyses based on the Dataset 1 showed that BI and ML trees harbored the same topologies. Both trees exhibited that *C. fieldii* of this study was made up of two major clades (I and II) with relatively strong supports (*PP* = 1.0, *BS* = 100) (Fig. 1: A), which were compatible with the haplotype median-joining network analysis (Fig. 1: B). Clade I contained 13 haplotypes from Shaanxi, Henan, Gansu, Anhui, Hubei, Sichuan, Qinghai, and some regions of Yunnan. Clade II consisted of five haplotypes from some regions of Yunnan and Tibet. Among 18 haplotypes, A7 and A2 of the population DL were detected in clades I and II, respectively. Clade I could be further divided into two subclades, each of which was not geographically specific, while clade II only contained one subclade (Fig. 1: A).

The comparison between the fixed indices N_{ST} and G_{ST} revealed an obvious correlation between phylogeny and geography. The N_{ST} value (0.63323) was much larger than the G_{ST} value (0.18432) ($P < 0.01$), indicating the existence of a significant phylogeographic structure. The reconstructed haplotype median-joining network showed that the haplotype A7 was probably the ancestral haplotype of clade I, which subsequently diverged into two subclades (A3, A4, A7, A10 and A13; A5, A6, A8, A11, A9, A12, A15 and A1, respectively), with A3, A7 and A15 being the shared haplotypes by some populations. The haplotype A16 should be considered as the ancestral haplotype of

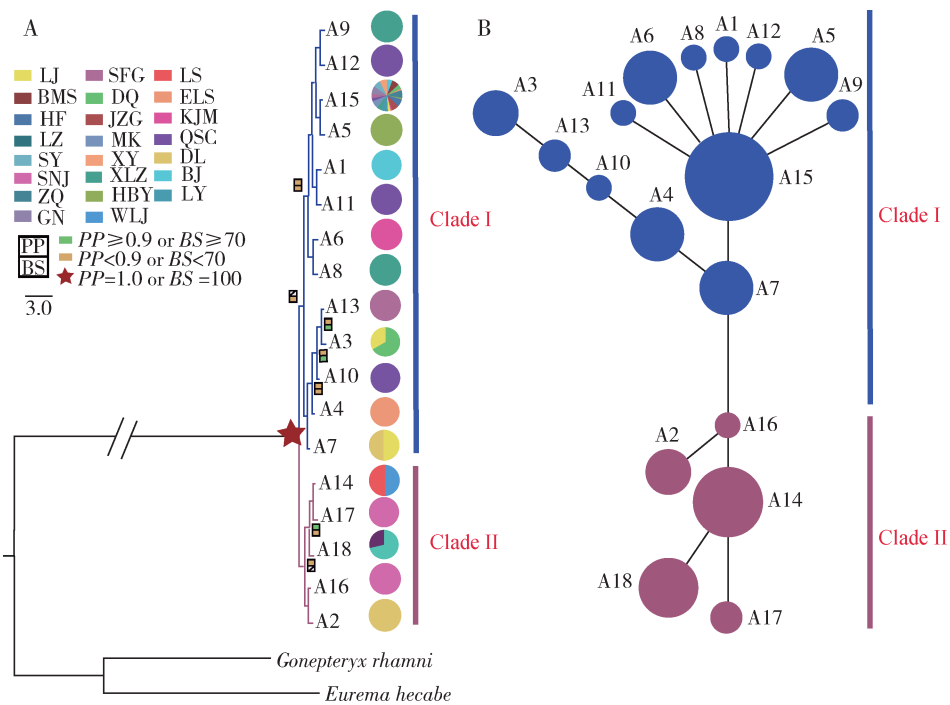

Fig. 1　Phylogenetic tree (A) of all the haplotypes of the concatenated sequence of mitochondrial genes *COI*, *Cytb*, *NDI* and *ND5* of *Colias fieldii* populations in China inferred using both maximum likelihood (ML) and Bayesian inference (BI) methods and haplotype median-joining network (B)

Bootstrap values (*BS*) lower than 50 and posterior probabilities (*PP*) lower than 0.5 were not shown. Haplotypes are represented as pie-diagrams with the slice-size proportional to the number of individuals as detailed in Table 1. A1 – A18: Haplotypes 1 – 18.

clade II, with A14 and A18 shared each by two populations. Of all the populations in this study, populations from Yunnan had the highest number of haplotypes, with A15 being the most widely distributed one.

3.3 Population differentiation

The results of analysis of AMOVA showed that the genetic variation among and within populations were 64.36% and 35.64%, respectively, indicating a larger population differentiation between the two clades of *C. fieldii* and a subtle differentiation within each clade (Table 4). Meanwhile, the genetic differentiation coefficient (F_{ST}) of the total population was 0.608, and the gene flow (Nm) of the total population was 0.160, indicating high population genetic differentiation ($F_{ST} > 0.250$) and relatively limited gene flow ($Nm < 1.000$). The F_{ST} and Nm values between the two clades were 0.632 and 0.140, respectively. In addition, the calculated haplotype diversity (Hd) and nucleotide diversity (π) of clade I were 0.511 ± 0.064 and 0.00041 ± 0.00008, respectively, and those of clade II were 0.723 ± 0.062 and 0.00046 ± 0.00008, respectively.

Table 4 Analysis of molecular variance (AMOVA) of different *Colias fieldii* populations in China based on the concatenated sequence of mitochondrial genes *COI*, *Cytb*, *NDI* and *ND5*

Source of variation	*d.f.*	Sum of squares	Variance components	Percentage of variation
Among populations	1	35.311	0.94531 *	64.36
Within population	113	59.141	0.52337 *	35.64
Total	114	94.452	1.46869 *	

* $P < 0.001$.

3.4 Demographic history

Demographic analysis based on the concatenated sequence of mitochondrial genes *COI*, *Cytb*, *NDI* and *ND5* showed that the two clades I and II of *C. fieldii* populations have undergone different demographic histories. The un-unimodal mismatch distribution and non-significantly negative Tajima's *D* value indicated that no obvious population expansion events happened in populations with haplotypes in clade I (Table 5). Demographic expansion of populations with haplotypes in clade II was confirmed by the significantly negative Fu's *Fs* value ($Fs = -28.963$, $P = 0$), although Tajima's *D* value ($D = 0.160$, $P > 0.10$) was non-significantly positive. The mismatch distribution was unimodal (Fig. 2) and both SSD and HRI index tests failed to reject the hypothesis of a sudden expansion model (Ramos-Onsins and Rozas, 2002; Excoffier, 2004; Li *et al.*, 2016).

Table 5 Results of neutrality test and mismatch analyses of *Colias fieldii* populations in China with haplotypes in clades I and II based on the concatenated sequence of mitochondrial genes *COI*, *Cytb*, *NDI* and *ND5*

Parameter	Clade I	Clade II
Tajima's *D*	−1.390	0.160
Fu's *Fs*	−30.089 *	−28.963 *
SSD	0.00316	0.00288
HRI	0.09102	0.07802
Tau (95% CI)	0.090 (0.000 − 2.314)	1.242 (0.623 − 2.172)

Clade I contained 13 haplotypes (A3, A4, A7, A10, A13, A5, A6, A8, A11, A9, A12, A15 and A1) from Shaanxi, Henan, Gansu, Anhui, Hubei, Sichuan, Qinghai, and some regions of Yunnan. Clade II contained five haplotypes (A2, A14, A16, A17 and A18) from some regions of Yunnan and Tibet. The same below. SSD: Sum of squared deviation; HRI: Harpending's raggedness index; * Significance at $P < 0.05$.

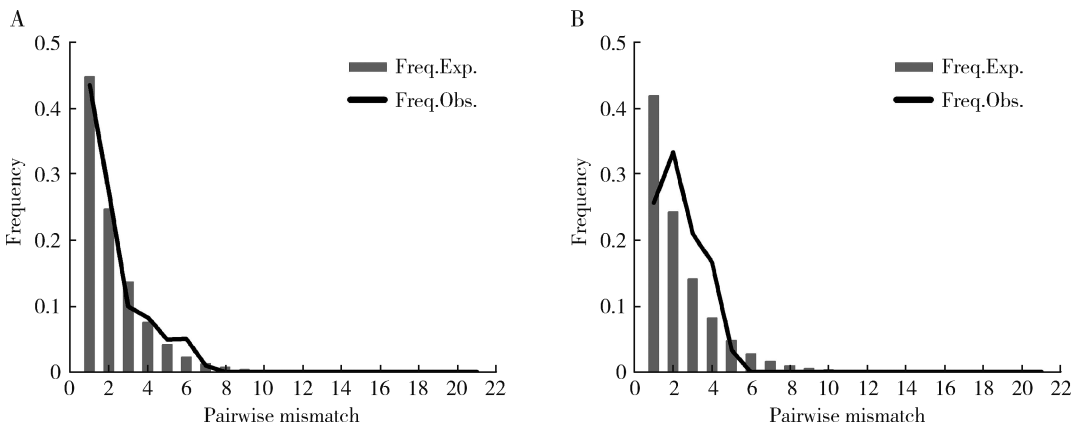

Fig. 2 Pairwise mismatch distributions of *Colias fieldii* populations in China with haplotypes in clades I (A) and II (B) based on the concatenated sequence of mitochondrial genes *COI*, *Cytb*, *NDI* and *ND5*

Freq. Obs. and Freq. Exp. represent the observed and expected mismatch distributions of a stationary population, respectively.

3.5 Divergence time estimation

Our molecular dating results indicated that the first divergence between the subfamilies Coliadinae and Pierinae originated at about 86.22 Ma [95% confidence interval (CI) = 83.33 − 89.27 Ma] in the Late Cretaceous (Santonian), and the two subfamilies began to diverge at about 64.75 Ma (95% CI = 52.15 − 77.73 Ma) and 66.84 Ma

(95% CI = 55.29 – 77.87 Ma) during the Late Cretaceous and the early Paleocene, respectively. For *C. fieldii*, the divergence time of the two evolutionary clades (clades I and II) occurred at about 0.48 Ma (95% CI = 0.24 – 0.74 Ma) during the middle Pleistocene (Fig. 3). Based on the value of τ and substitution rate of 0.73×10^{-9} per site per year for four mitochondrial genes, the demographic expansion time of clade II was estimated at approximately 0.085 Ma during the Late Pleistocene.

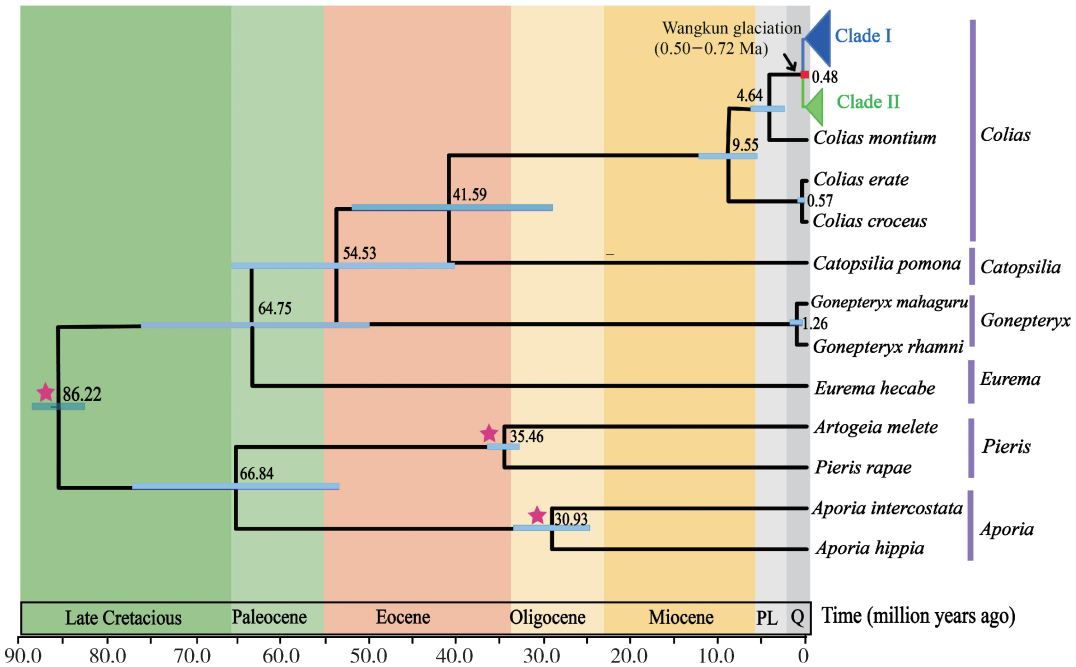

Fig. 3　Evolutionary timescale of the *Colias fieldii* populations in China estimated by relaxed molecular dating method based on the concatenated sequence of mitochondrial genes *COI*, *Cytb*, *NDI* and *ND5*

Origin species of *COI*, *Cytb*, *NDI* and *ND5* and their GenBank accession numbers: *Colias montium*, MN305669, MN305670, KM669350, MN305671; *Colias erate*, KP715146, KP715146, KP715146, KP715146; *Colias croceus*, KM592967, KM592967, KM592967, KM592967; *Catopsilia pomona*, DQ842501, JX274649, GU462136, JX274649; *Gonepteryx mahaguru*, GU372557, KF881048, KF881048, KF881048; *Gonepteryx rhamni*, MF536894, MF536894, MF536894, MF536894; *Eurema hecabe*, KC257480, KC257480, KC257480, KC257480; *Artogeia melete*, EU597124, EU597124, EU597124, EU597124; *Pieris rapae*, GQ398376, GQ398376, GQ398376, GQ398376; *Aporia intercostata*, KC461928, KC461928, KC461928, KC461928; *Aporia hippia*, KX495166, KX495166, KX495166, KX495166. The confidence intervals are shown by blue bars on the phylogram and fossil calibration points shown by red asterisks. Q: Quaternary, PL: Pliocene.

4　DISCUSSION

4.1　Genetic diversity and population differentiation

Nucleotide and haplotype diversities can provide information about an organism's population structure and history. Our results revealed that *C. fieldii* had a relatively high level of haplotype diversity ($Hd > 0.500$) and a low level of nucleotide diversity ($\pi < 0.005$) (Grant and Bowen, 1998). In addition, the values of haplotype and nucleotide diversities of clade I were lower than those of clade II, and the fact might be attributed to the genetic drift or inbreeding depression among clade I populations or individuals. Furthermore, the genetic differentiation between the two clades I and II was mainly associated with a wide range of ecological types, as well as the complex mountain barriers (niche variations) (Slatkin and Maddison, 1989; Wright, 1990).

The haplotype analysis showed that among all the geographic populations of *C. fieldii*, the Yunnan population possessed the most haplotypes, including the unique and the most broadly distributed ones, such as haplotypes A7 and A15. The fact suggests that the southwestern Yunnan area probably be the diversification centre of *C. fieldii* in China, which is in agreement with the common view that the Hengduan Mountains is one of the most significant biodiversity hotspots in the world, with high levels of species richness and endemism (Yang *et al.*, 2009; Che *et al.*, 2010; Song *et al.*, 2010; Liao *et al.*, 2016). However, more genetic differentiation analyses are needed to better understand the way in which palaeogeographical and palaeoclimatic events shaped the distribution and phylogeographical patterns of *C. fieldii* populations. The small sample size of this study is also one of the reasons for this result, so we need to examine more populations in the future.

4.2 Divergence time estimation

Our phylochronological results (Fig. 3) generally agreed with those of Braby *et al.* (2005), Braby and Trueman (2006) and Cao *et al.* (2016), who determined the divergence between Coliadinae and Pierinae dated at about 86.34 Ma (95% CI = 83.59 – 88.83 Ma) in the Late Cretaceous, but significantly differed from the results obtained by Dong *et al.* (2019), who provided dates of the same event at about 71.5 Ma (95% CI = 93.6 – 49.4 Ma) (Late Cretaceous). We found that the major source of differences in dating the tree came from calibration points and their distribution in the tree. In this analysis, we adopted, in our calibration system (Fig. 3), high-quality fossil dates of *Pieris* and *Aporia* and relevant dates from the host-plants (Brassicales) based on the insect-host plant coevolutionary scenario, which were likely better proxies approaching the true reference time frame. Therefore, the divergence time in this study might be earlier than the divergence time estimated without the restriction of host plant fossils. Although the time obtained in this study was slightly different from the time proposed by other scholars, there was still a large range overlap for the time estimates of 95% confidence interval.

Our results revealed that the two clades of *C. fieldii* diverged at about 0.48 Ma during the longest interglacial time after the Quaternary Wangkun glacial period (0.50 – 0.72 Ma, according to marine isotope stages, MIS 16 – 20) (Cui *et al.*, 1998) and the Southeast Asia moonson happened about 0.57 – 0.48 Ma. This time of increasing warmness and wetness accompanied by mountain forest expansion might have driven some populations to disperse from the margin into the core area of QTP, which colonized at new suitable habitats. In addition, some populations later dispersed into other low-latitude areas due to the Quaternary glacial-interglacial cycle events and Southeast Asia monsoon. All these factors eventually caused the complete diversification of the two clades distributed at high- and low-altitudes. That is, the low-altitude populations should experience less isolation, while high-altitude populations were more isolated in general (Lu *et al.*, 2012). Additionally, the genetic differentiation of *C. fieldii* in this study caused by geographical isolation could be further reinforced and accumulated due to ecological divergence over time, and finally the two clades inhabited differently and evolved independently into two genetically diversified clades (Yan *et al.*, 2010; Zhan *et al.*, 2011).

Besides, an obvious phylogeographic structure of *C. fieldii* detected in this study is somewhat attributed to their relatively lower flight ability compared with other animals that harbor a stronger ability of movement (Gratton *et al.*, 2008; Wheat and Watt, 2008). In these cases, such a low dispersal capacity tends to cause the gene flows to decrease continuously, thus promoting the genetic divergences among populations.

4.3 Demographic history

Previous studies have shown that compared with the drastic climate oscillations and glacial cycles in Europe and North America (Hewitt, 2004; Schmitt, 2007), a relatively mild Pleistocene climate and lack of ice sheets were presented in many areas of East Asia (Ju *et al.*, 2007). Population expansion of many species in Europe and North America usually occurred after LGM (Last Glacial Maximum), while the population expansions of many widespread species occurred before LGM in East Asia (Huang *et al.*, 2010). Our study showed that the two clades of *C. fieldii* might have taken different pathways in their evolutionary histories: clade II experienced an obvious population expansion event at about 0.085 Ma in the late Pleistocene interglacial period before the LGM, while clade I did not show any signs of population expansion. Thus, the demographic expansion of clade II during this period was consistent with previous reports concerning some birds and mammals in East Asia, such as the Chinese bamboo partridge *Bambusicola thoracica* (Huang *et al.*, 2010), Chinese hwamei *Leucodioptron canorum* (Li *et al.*, 2009), and tufted deer *Elaphodus cephalophus* (Sun *et al.*, 2016).

The high haplotype diversity and low nucleotide diversity also indicated that the clade II of *C. fieldii* might have undergone a rapid population expansion and accumulation of variation after the bottleneck effect. Accordingly, the discordance in evolutionary histories of the two clades of *C. fieldii* could be accounted for the differentiation of habitat distributions. During the extensive Pleistocene glaciation period, most regions of Qinghai and Tibet might have been heavily covered with ice, but the plain areas remained relatively ice-free, under which condition milder climate might have mitigated demographic stresses for the populations of plain areas relative to the extremes experienced by the QTP populations (Zhang *et al.*, 2000; Qu *et al.*, 2010). Additionally, these different evolutionary histories were probably caused by the different environmental events they experienced, that is, during late Pleistocene interglacial period (MIS5), the reinforced winter monsoon and decreased heavy

rainfall on the core plateau synergistically promoted the population expansion of clade II. Similar cases were also reported in birds, plants, and other insects (Wang *et al.*, 2010; Lei *et al.*, 2014; Ye *et al.*, 2016).

References

Bandelt HJ, Forster P, Röhl A, 1999. Median-joining networks for inferring intraspecific phylogenies. *Mol. Biol. Evol.*, 16(1): 37 – 48.

Braby MF, Trueman JWH, 2006. Evolution of larval host plant associations and adaptive radiation in pierid butterflies. *J. Evol. Biol.*, 19(5): 1677 – 1690.

Braby MF, Trueman JWH, Eastwood R, 2005. When and where did troidine butterflies (Lepidoptera: Papilionidae) evolve? Phylogenetic and biogeographic evidence suggests an origin in remnant Gondwana in the Late Cretaceous. *Invertebr. Syst.*, 19(2): 113 – 143.

Braby MF, Vila R, Pierce NE, 2006. Molecular phylogeny and systematics of the Pieridae (Lepidoptera: Papilionoidea): higher classification and biogeography. *Zool. J. Linn. Soc.*, 147(2): 239 – 275.

Cameron SL, 2014. Insect mitochondrial genomics: implications for evolution and phylogeny. *Annu. Rev. Entomol.*, 59: 95 – 117.

Cao M, Jin Y, Liu N, Ji W, 2012. Effects of the Qinghai-Tibetan Plateau uplift and environmental changes on phylogeographic structure of the Daurian Partridge (*Perdix dauuricae*) in China. *Mol. Phylogenet. Evol.*, 65(3): 823 – 830.

Cao Y, Hao JS, Sun XY, Zheng B, Yang Q, 2016. Molecular phylogenetic and dating analysis of pierid butterfly species using complete mitochondrial genomes. *Genet. Mol. Res.*, 15(4): gmr15049196.

Carneiro J, Sampaio I, Silva-Júnior JS, Farias IP, Hrbek T, Pissinatti A, Schneider H, 2018. Phylogeny, molecular dating and zoogeographic history of the titi monkeys (*Callicebus*, Pitheciidae) of eastern Brazil. *Mol. Phylogenet. Evol.*, 124: 10 – 15.

Che J, Zhou WW, Hu JS, Yan F, Papenfuss TJ, Wake DB, Zhang YP, 2010. Spiny frogs (Paini) illuminate the history of the Himalayan region and Southeast Asia. *Proc. Natl. Acad. USA*, 107(31): 13765 – 13770.

Cristiano MP, Cardoso DC, Fernandes-Salomão TM, Heinze J, 2016. Integrating paleodistribution models and phylogeography in the grass-cutting ant *Acromyrmex striatus* (Hymenoptera: Formicidae) in southern lowlands of South America. *PLoS ONE*, 11(1): e0146734.

Cui Z, Wu Y, Liu G, Ge D, Pang Q, Xu Q, 1998. On Kunlun-Yellow River tectonic movement. *Sci. China* (*Ser. D*), 41(6): 592 – 600.

Darriba D, Taboada GL, Doallo R, Posada D, 2012. jModelTest 2: more models, new heuristics and parallel computing. *Nat. Methods*, 9(8): 772.

Ding C, Zhang Y, 2017. Phylogenetic relationships of Pieridae (Lepidoptera: Papilionoidea) in China based on seven gene fragments. *Entomol. Sci.*, 20(1): 15 – 23.

Dong SY, Jiang GF, Liu G, Hong F, Hsu Y, 2019. The complete mitochondrial genome of the Golden Birdwing butterfly *Troides aeacus*: insights into phylogeny and divergence times of the superfamily Papilionoidea. *BioRxiv*, 2019: 529347.

Drummond AJ, Rambaut A, 2007. BEAST: Bayesian evolutionary analysis by sampling trees. *BMC Evol. Biol.*, 7(1): 214.

Eckert AJ, Tearse BR, Hall BD, 2008. A phylogeographical analysis of the range disjunction for foxtail pine (*Pinus balfouriana*, Pinaceae): the role of Pleistocene glaciation. *Mol. Ecol.*, 17(8): 1983 – 1997.

Excoffier L, 2004. Patterns of DNA sequence diversity and genetic structure after a range expansion: lessons from the infinite-island model. *Mol. Ecol.*, 13(4): 853 – 864.

Excoffier L, Lischer HEL, 2010. Arlequin suite ver 3.5: a new series of programs to perform population genetics analyses under Linux and Windows. *Mol. Ecol. Resour.*, 10(3): 564 – 567.

Favre A, Päckert M, Pauls SU, Jähnig SC, Uhl D, Michalak I, Muellnerriehl-Riehl AN, 2015. The role of the uplift of the Qinghai-Tibetan Plateau for the evolution of Tibetan biotas. *Biol. Rev. Camb. Philos. Soc.*, 90(1): 236 – 253.

Fu YX, 1997. Statistical tests of neutrality of mutations against population growth, hitchhiking and background selection. *Genetics*, 147(2): 915 – 925.

Galtier N, Nabholz B, Glémin S, Hurst GDD, 2009. Mitochondrial DNA as a marker of molecular diversity: a reappraisal. *Mol. Ecol.*, 18(22): 4541 – 4550.

Grant W, Bowen BW, 1998. Shallow population histories in deep evolutionary lineages of marine fishes: insights from sardines and anchovies and lessons for conservation. *J. Hered.*, 89(5): 415 – 426.

Gratton P, Konopiński MK, Sbordoni V, 2008. Pleistocene evolutionary history of the Clouded Apollo (*Parnassius mnemosyne*): genetic signatures of climate cycles and a 'time-dependent' mitochondrial substitution rate. *Mol. Ecol.*, 17(19): 4248 – 4262.

Harpending HC, 1994. Signature of ancient population growth in a low-resolution mitochondrial DNA mismatch distribution. *Hum. Biol.*, 66(4): 591 – 600.

He HY, Yu WD, Jiang WB, 2016. Research progress in mitochondrial genomics of butterflies. *Chin. Bull. Life Sci.*, 28(9): 978 – 985. [何海燕, 俞伟东, 蒋韦斌, 2016. 蝶类线粒体基因组学研究进展. 生命科学, 28(9): 978 – 985]

Hewitt GM, 2004. Genetic consequences of climatic oscillations in the Quaternary. *Philos. Trans. R. Soc. Lond. B*, 359(1442): 183 – 195.

Huang Z, Liu N, Liang W, Zhang Y, Liao X, Ruan L, Yang Z, 2010. Phylogeography of Chinese bamboo partridge, *Bambusicola thoracica thoracica* (Aves: Galliformes) in south China: inference from mitochondrial DNA control-region sequences. *Mol. Phylogenet. Evol.*, 56(1): 273 – 280.

Huelsenbeck JP, Ronquist F, 2001. MrBayes: Bayesian inference of phylogenetic trees. *Bioinformatics*, 17(8): 754 – 755.

Ju L, Wang H, Jiang D, 2007. Simulation of the Last Glacial Maximum climate over East Asia with a regional climate model nested in a general circulation model. *Palaeogeogr. Palaeocl. Palaeoecol.*, 248(3 – 4): 376 – 390.

Katoh K, Rozewicki J, Yamada KD, 2017. MAFFT online service: multiple sequence alignment, interactive sequence choice and visualization. *Brief. Bioinform.*, 20(4): 1160 – 1166.

Kumar S, Stecher G, Tamura K, 2016. MEGA7: molecular evolutionary genetics analysis version 7.0 for bigger datasets. *Mol. Biol. Evol.*, 33(7): 1870 – 1874.

Laiho J, Ståhls G, 2013. DNA barcodes identify Central Asian *Colias* butterflies (Lepidoptera, Pieridae). *ZooKeys*, 365(365): 175 – 196.

Lei F, Qu Y, Song G, 2014. Species diversification and phylogeographical patterns of birds in response to the uplift of the Qinghai-Tibet Plateau and Quaternary glaciations. *Curr. Zool.*, 60(2): 149 – 161.

Li SH, Yeung CKL, Feinstein J, Han L, Le MH, Wang CX, Ding P, 2009. Sailing through the Late Pleistocene: unusual historical demography of an East Asian endemic, the Chinese Hwamei (*Leucodioptron canorum canorum*), during the last glacial period. *Mol. Ecol.*, 18(4): 622 – 633.

Li XB, Tang QY, Yu D, Liu HZ, 2016. Genetic diversity and population history of longnose gudgeon (*Saurogobio dabryi*) in the upper Yangtze River and Chishui River based on cytochrome b gene sequences. *Chin. J. Zool.*, 51(5): 833 – 843. [李小兵, 唐琼英, 俞丹, 刘焕章, 2016. 长江上游干流及赤水河蛇鮈遗传多样性与种群历史分析. 动物学杂志, 51(5): 833 – 843]

Li Z, Yu G, Rao D, Yang J, 2012. Phylogeography and demographic history of *Babina pleuraden* (Anura, Ranidae) in southwestern China. *PLoS ONE*, 7(3): e34013.

Liao J, Jing D, Luo G, Wang Y, Zhao L, Liu N, 2016. Comparative phylogeography of *Meriones meridianus*, *Dipus sagitta*, and *Allactaga sibirica*: potential indicators of the impact of the Qinghai-Tibetan Plateau uplift. *Mamm. Biol.*, 81(1): 31 – 39.

Librado P, Rozas J, 2009. DnaSP v5: a software for comprehensive analysis of DNA polymorphism data. *Bioinformatics*, 25(11): 1451 – 1452.

Lu B, Zheng Y, Murphy RW, Zeng X, 2012. Coalescence patterns of endemic Tibetan species of stream salamanders (Hynobiidae: *Batrachuperus*). *Mol. Ecol.*, 21(13): 3308 – 3324.

Meng YF, Shang SQ, Zhang YL, 2013. The morphology of the reproductive system of *Colias fieldii*. *Chin. J. Appl. Entomol.*, 50(3): 813 – 817. [孟银凤, 尚素琴, 张雅林, 2013. 橙黄豆粉蝶生殖系统形态学研究. 应用昆虫学报, 50(3): 813 – 817]

Nguyen LT, Schmidt HA, von Haeseler A, Minh BQ, 2014. IQ-TREE: a fast and effective stochastic algorithm for estimating maximum-likelihood phylogenies. *Mol. Biol. Evol.*, 32(1): 268 – 274.

Pons O, Petit RJ, 1996. Measuring and testing genetic differentiation with ordered versus unordered alleles. *Genetics*, 144(3): 1237 – 1245.

Qu Y, Lei F, Zhang R, Lu X, 2010. Comparative phylogeography of five avian species: implications for Pleistocene evolutionary history in the Qinghai-Tibetan plateau. *Mol. Ecol.*, 19(2): 338 – 351.

Rambaut A, 2009. FigTree v1.4: Tree Figure Drawing Tool. Available from: http://treebioedacuk/software/figtree/.

Rambaut A, Drummond AJ, Xie D, Baele G, Suchard MA, 2018. Posterior summarization in Bayesian phylogenetics using Tracer 1.7. *Syst. Biol.*, 67(5): 901 – 904.

Ramos-Onsins SE, Rozas J, 2002. Statistical properties of new neutrality tests against population growth. *Mol. Biol. Evol.*, 19(12): 2092 – 2100.

Rogers AR, Harpending H, 1992. Population growth makes waves in the distribution of pairwise genetic differences. *Mol. Biol. Evol.*, 9(3): 552 – 569.

Ronquist F, Huelsenbeck JP, 2003. MrBayes 3: Bayesian phylogenetic inference under mixed models. *Bioinformatics*, 19(12): 1572 – 1574.

Schmitt T, 2007. Molecular biogeography of Europe: Pleistocene cycles and postglacial trends. *Front. Zool.*, 4(1): 11.

Schoville SD, Stuckey M, Roderick GK, 2011. Pleistocene origin and population history of a neoendemic alpine butterfly. *Mol. Ecol.*, 20(6): 1233 – 1247.

Scudder SH, 1875. Fossil butterñies. *Mem. Am. Assoc. Adv. Sci.*, 1: 1 – 99.

Scudder SH, 1889. The fossil butterñies of Florissant. US Geological Survey, 8th Annual Report Part I. 433 – 474.

Simon C, Frati F, Beckenbach A, Beckenbach AT, Crespi B, Liu H, Flook P, 1994. Evolution, weighting, and phylogenetic utility of mitochondrial gene sequences and a compilation of conserved polymerase chain reaction primers. *Ann. Entomol. Soc. Am.*, 87(6): 651 – 701.

Slatkin M, Maddison WP, 1989. A cladistic measure of gene flow inferred from the phylogenies of alleles. *Genetics*, 123(3): 603 – 613.

Song JH, Kang HS, Byun YH, Hong SY, 2010. Effects of the Tibetan Plateau on the Asian summer monsoon: a numerical case study using a regional climate model. *Int. J. Climatol.*, 30(5): 743 – 759.

Su C, Shi Q, Sun X, Ma J, Li C, Hao J, Yang Q, 2017. Dated phylogeny and dispersal history of the butterfly subfamily Nymphalinae (Lepidoptera: Nymphalidae). *Sci. Rep.*, 7(1): 8799.

Sun Z, Pan T, Wang H, Pang M, Zhang B, 2016. Yangtze River, an insignificant genetic boundary in tufted deer (*Elaphodus cephalophus*): the evidence from a first population genetics study. *PeerJ.*, 4(9): e2654.

Tajima F, 1989. Statistical method for testing the neutral mutation hypothesis by DNA polymorphism. *Genetics*, 123(3): 585 – 595.

Tao R, Xu C, Wang Y, Sun X, Li C, Ma J, Hao J, Yang Q, 2020. Spatiotemporal differentiation of Alpine butterfly *Parnassius glacialis* (Papilionidae: Parnassiinae) in China: evidence from mitochondrial DNA and nuclear single nucleotide polymorphisms. *Genes*, 11(2): 188.

Wang H, Qiong L, Sun K, Lu F, Wang Y, Song Z, Zhang W, 2010. Phylogeographic structure of *Hippophae tibetana* (Elaeagnaceae) highlights the highest microrefugia and the rapid uplift of the Qinghai-Tibetan Plateau. *Mol. Ecol.*, 19(14): 2964 – 2979.

Wheat CW, Watt WB, 2008. A mitochondrial-DNA-based phylogeny for some evolutionary-genetic model species of *Colias* butterflies (Lepidoptera: Pieridae). *Mol. Phylogenet. Evol.*, 47(3): 893 – 902.

Wright S, 1990. Evolution in Mendelian populations. *Bull. Math. Biol.*, 52(1 – 2): 241 – 295.

Xia X, 2017. DAMBE6: new tools for microbial genomics, phylogenetics, and molecular evolution. *J. Hered.*, 108(4): 431 – 437.

Yagi T, Sasaki G, Takebe H, 1999. Phylogeny of Japanese papilionid butterflies inferred from nucleotide sequences of the mitochondrial *ND5* gene. *J. Mol. Evol.*, 48(1): 42 – 48.

Yan J, Wang Q, Chang Q, Ji X, Zhou K, 2010. The divergence of two independent lineages of an endemic Chinese gecko, *Gekko swinhonis*, launched by the Qinling orogenic belt. *Mol. Ecol.*, 19(12): 2490 – 2500.

Yang F, Ignatieva M, Wissman J, Ahrné K, Zhang S, Zhu S, 2019. Relationships between multi-scale factors, plant and pollinator diversity, and composition of park lawns and other herbaceous vegetation in a fast growing megacity of China. *Landsc. Urban Plan.*, 185: 117 – 126.

Yang S, Dong H, Lei F, 2009. Phylogeography of regional fauna on the Tibetan Plateau: a review. *Prog. Nat. Sci.*, 19(7): 789 – 799.

Ye Z, Chen P, Bu W, 2016. Terrestrial mountain islands and Pleistocene climate fluctuations as motors for speciation: a case study on the genus *Pseudovelia* (Hemiptera: Veliidae). *Sci. Rep.*, 6(1): 33625.

You Y, Sun K, Xu L, Wang L, Jiang T, Liu S, Lu G, Berquist SW, Feng J, 2010. Pleistocene glacial cycle effects on the phylogeography of the Chinese endemic bat species, *Myotis davidii*. *BMC Evol. Biol.*, 10(1): 208.

Zhan X, Zheng Y, Wei F, Bruford MW, Jia C, 2011. Molecular evidence for Pleistocene refugia at the eastern edge of the Tibetan Plateau. *Mol. Ecol.*, 20(14): 3014 – 3026.

Zhang D, Fengquan L, Jianmin B, 2000. Eco-environmental effects of the Qinghai-Tibet Plateau uplift during the Quaternary in China. *Environ. Geol.*, 39(12): 1352 – 1358.

Zhang SQ, Che LH, Li Y, Liang D, Pang H, Ślipiński A, Zhang P, 2018. Evolutionary history of Coleoptera revealed by extensive sampling of genes and species. *Nat. Commun.*, 9(1): 205.

Zheng D, 1996. The system of physico-geographical regions of the Qinghai-Xizang (Tibet) Plateau. *Sci. China.* (*Ser. D*), 39(4): 410 – 417.

Zhou S, Wang X, Wang J, Xu L, 2006. A preliminary study on timing of the oldest Pleistocene glaciation in Qinghai-Tibetan Plateau. *Quatern. Int.*, 154: 44 – 51.

基于线粒体基因序列的中国橙黄豆粉蝶遗传分化和谱系生物地理研究

陈可可[1]，罗阿蓉[2]，王运良[1]，司成才[1]，黄敦元[3]，苏成勇[1]，郝家胜[1,*]，朱朝东[2,*]

（1. 安徽师范大学生命科学学院，安徽芜湖 241000；2. 中国科学院动物研究所，动物系统学与进化重点实验室，北京 100101；3. 重庆师范大学生命科学学院，重庆 401331）

摘要：【目的】分析中国橙黄豆粉蝶 *Colias fieldii* 种群遗传多样性和遗传分化情况及其系统发生关系，推测其起源及分化时间，并探讨其历史生物地理分布格局的成因。【方法】对 2006－2018 年采集的中国 23 个橙黄豆粉蝶地理种群的 115 头个体样品的 4 个线粒体基因（*COI*，*Cytb*，*NDI* 和 *ND5*）序列进行 PCR 扩增和测序；采用 MEGA v.7.0，DnaSP v.5.0 和 Arlequin v.3.5.1 等软件分析其遗传多样性和遗传分化情况；以其他近缘豆粉蝶种类作为外类群，采用 IQ-TREE，MrBayes v.3.1.2，Network v.4.6 和 BEAST v.1.8.3 等软件重建橙黄豆粉蝶的系统发生树和单倍型网络图，并使用宽松分子钟以及前人的时间标定推测橙黄豆粉蝶的起源和分化时间；结合现今橙黄豆粉蝶的生物地理分布特点和第四纪以来的地球环境背景，探讨其历史生物地理分布格局及成因。【结果】橙黄豆粉蝶种群 4 个线粒体基因（*COI*，*Cytb*，*NDI* 和 *ND5*）片段长度分别为 648，699，393 和 777 bp，这 4 个基因的串联序列总长为 2 517 bp，具有明显的 AT 偏倚特征。基于 4 个线粒体基因序列，供试橙黄豆粉蝶 23 个地理种群 115 头个体中共检测出 18 个单倍型，总群体的单倍型多样性（*Hd*）和核苷酸多样性（π）分别为 0.677 ±0.048 和 0.00066 ±0.00007，呈现出较高的单倍型多样性和较低的核苷酸多样性。系统发育分析表明，橙黄豆粉蝶种群的 18 个单倍型分为 2 个具有明显地理分布格局的支系（Ⅰ和Ⅱ），支系Ⅰ包含 13 个单倍型，主要来自陕西、河南、甘肃、安徽、湖北、四川、青海及云南部分地区的种群；支系Ⅱ由 5 个单倍型组成，主要来自云南部分地区及西藏的种群；单倍型网络图与系统发生树结果一致。AMOVA 分析结果表明，大部分的种群遗传分化（64.36%）来自于橙黄豆粉蝶种群两单倍型支系间，各分支内的遗传分化较小（35.64%）。中性检验和错配分布分析结果显示，单倍型支系Ⅰ的种群未发生过种群扩张事件，而单倍型支系Ⅱ的种群在历史上发生过种群扩张事件，扩张事件发生的时间（0.085 Ma）位于末次冰盛期前的间冰期，这一结果可能是由于间冰期温暖湿润的高原气候以及森林草原扩张、强降雨减少等因素造成的。【结论】橙黄豆粉蝶种群的遗传分化与地理距离之间存在明显的相关性。其祖先可能在距今 48 万年前起源于我国的西南地区（现今横断山区一带），之后，由于第四纪冰期-间冰期轮回事件、东南亚季风以及栖息地环境的影响而分化为 2 大支系并逐渐向低海拔地区扩散。

关键词：橙黄豆粉蝶；遗传分化；单倍型；线粒体基因；分子年代测定；谱系生物地理学；中国

中图分类号：Q963　　**文献标识码：**A　　**文章编号：**0454-6296（2020）12-1525-11

（责任编辑：马丽萍）